59th ILMENAU SCIENTIFIC COLLOQUIUM
Technische Universität Ilmenau, 11 — 15 September 2017
URN: urn:nbn:de:gbv:ilm1-2017iwk-047:1

MULTI-SEGMENTED ARTIFICIAL LOCOMOTION SYSTEMS WITH ADAPTIVELY CONTROLLED GAIT TRANSITIONS

Jonas Krämll / Carsten Behn

Technical Mechanics Group, Department of Mechanical Engineering
Technische Universität Ilmenau
Max-Planck-Ring 12, 98693 Ilmenau, Germany
{jonas.kraeml, carsten.behn}@tu-ilmenau.de

ABSTRACT

This paper is devoted to the analysis and simulation of multi-segmented artificial locomotion systems. The biological paradigm is the earthworm. Here, we restrict our investigation to a crawling system which is moving along a straight line, more precisely, the system is firstly moving unidirectionally. Recent results from the examined literature present investigations of short worms ($n < 4$). In contrast to this, the developed mechanical model in this paper consists of a chain of 10 discrete mass points. Let us point out, that the presented investigations are not restricted to a fixed number of mass points. To achieve a movement of the system, the distances between neighboring mass points are controlled by viscoelastic force actuators. Due to a prescribed reference gait, an adaptive controller determines the necessary forces to adjust the prescribed values. Then, due shortening and lengthening of these distances together with a spiky ground contact at the mass point (preventing velocities from being negative), we achieve a global movement of the whole system – called undulatory locomotion. Specific prescribed gaits are required to guarantee a controlled movement that differ especially in the number of resting mass points and the load of actuators and spikes. To determine the most advantageous gaits, numerical investigations are performed and a weighting function offers a decision of best possible gaits. Finally, a gait transition algorithm for an autonomously change of the locomotion velocity and number of resting mass points in dependence on the spike and actuator force load is presented and tested in numerical simulations.

Index Terms— artificial locomotion system, optimal gait, gait transition algorithm, adaptive control.

1. INTRODUCTION

In current mechanics literature, worm-like locomotion systems play an increasing role, see for example [1–5], and also are part of teaching and education of students, see textbooks [6,7]. The advantage of these systems is their little space requirements due to their unidirectional motion. Therefore, they are used in environments that are difficult to access for humans or other motion systems. Possible applications are, e.g., minimally invasive surgery [8], service and maintenance robots [9] or drilling robots [10].
Previous publications deal with worm-like locomotion systems with 3 or 4 mass points [11]. This paper increases the knowledge of worm-like locomotion by the dynamic behavior of systems with 10 mass points with the goal to expand the gained results to snake-like locomotion systems in further works.
First of all, the mechanical model of a worm-like locomotion system and the adaptive control scheme are presented. Afterwards, the generation of suitable gaits considering current literature is introduced. These gaits are used by a gait transition algorithm that changes velocity and number of resting mass points depending on the load of spikes and actuators, like the biological paradigm does [12]. Finally, simulations are carried out to demonstrate the functionality of the scheme.

2. MODELING & CONTROL

The model is identical to [7]. The kinematic model comprises a chain of discrete mass points m_i as shown in Fig. 1, where $x_i(t)(i = 0 \dots n)$ are the coordinates of the mass points, which each own one degree of freedom. The

distance of neighboring mass elements is:

$$l_j(t) := x_{i-1}(t) - x_i(t) \tag{1}$$

Ideal spikes are mounted at each segment to inhibit backward movement.

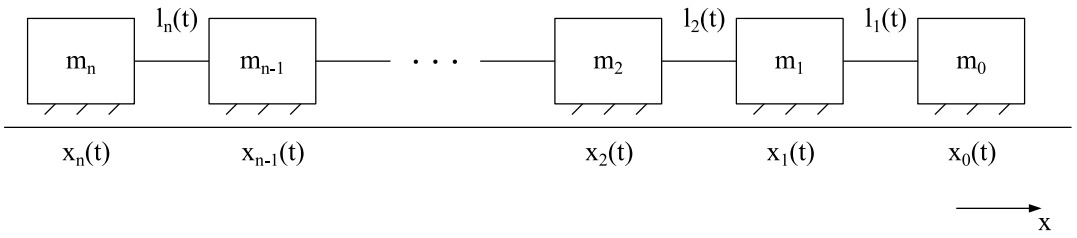

Figure 1: Chain of mass points with spikes, modified from [11].

In this model, a segment is a mass point, but it can also appear as balloon-like or bellows-like elements (possibly fluid filled), see [4, 5, 13, 14].
To allow a movement of the worm, the distances between the mass points have to be shortened and lengthened. This can be done in adjusting their longitudinal or radial dimensions [15] or, as here, the distances between adjacent elements [16, 17]. For this purpose, as a first purely theoretical realization, viscoelastic actuators are assumed between the segments in the dynamic model. The applied forces on a mass point are (as you can see in Fig. 2):

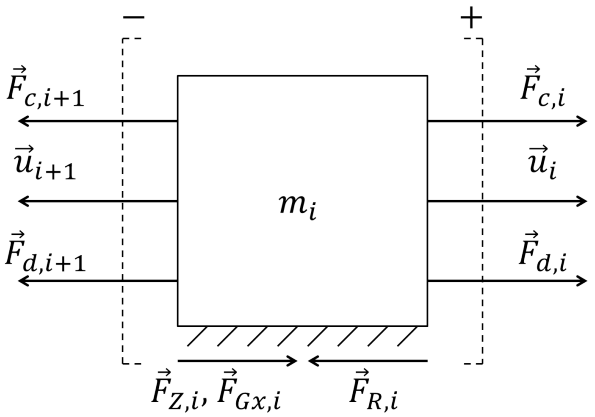

Figure 2: Mass point with forces, adapted from [11].

- spring forces $F_{c,i} = c_i(x_{i-1} - x_i - l_{0,i})$ and $F_{c,i+1} = -c_{i+1}(x_i - x_{i+1} - l_{0,i+1})$, where $l_{0,i}$ and $l_{0,i+1}$ are the detensioned lengths of the springs;
- damping forces $F_{d,i} = d_i(\dot{x}_{i-1} - \dot{x}_i)$ and $F_{d,i+1} = -d_{i+1}(\dot{x}_i - \dot{x}_{i+1})$;
- actuator forces u_i and u_{i+1};
- spike forces $F_{Z,i}$;
- weight $F_{Gx,i}$ in x-direction;
- friction force $F_{R,i} = 0$, like Stokes friction due to environmental contact.

Remark 2.1. *At this stage of investigations, the assumed zero friction force is only a special case. The interaction to the ground is modeled via ideal spikes. In future work, we will replace these spikes by anisotropic Coulomb friction, see also [7, 16, 17].*

According to [7], the ideal spikes have to fulfill these conditions:

$$\dot{x}_i \geq 0, \qquad F_{Z,i} \geq 0, \qquad \dot{x}_i \cdot F_{Z,i} = 0 \tag{2}$$

This complementary-slackness condition can be fulfilled by the following equation, where F_i is the sum of all remaining applied forces:

$$F_{Z,i} = -\frac{1}{2}\left[1 - \operatorname{sign}(\dot{x}_i)\right] \cdot \left[1 - \operatorname{sign}(F_i)\right] \cdot F_i \tag{3}$$

Using Newton's second law, the coupled differential equations for movement of the segments can be formulated:

$$\begin{aligned} m_i \ddot{x}_i = &+c_i(x_{i-1} - x_i - l_{0,i}) - c_{i+1}(x_i - x_{i+1} - l_{0,i+1}) \\ &+ d_i(\dot{x}_{i-1} - \dot{x}_i) - d_{i+1}(\dot{x}_i - \dot{x}_{i+1}) \\ &+ u_i - u_{i+1} + F_{Z,i} + F_{Gx,i} + F_{R,i} \end{aligned} \tag{4}$$

with $c_0 = c_{n+1} = d_0 = d_{n+1} = u_0 = u_{n+1} = 0$. The DoF of the system is N.
To generate a movement of the system, acuators have to apply forces on the mass points. They serve as inputs to the crawling system to control the distances between the segments.

To follow a given motion pattern, to deal with unknown or uncertain system parameters and to react to changes of the environment, an adaptive controller is used that generates necessary actuator forces autonomously. The forces depend on the error $e_j(t)$:

- $l_j(t) := x_{j-1}(t) - x_j(t)$, the distance between neighboring mass points, which are the system outputs;
- $l_{ref,j}(t)$, the predefined time-variant reference distance functions, i.e., a later determined optimal motion pattern in form of a kinematic gait;
- $e_j(t) := l_j(t) - l_{ref,j}(t)$, error of the output.

The used controller is described in [18]. It contains regular PD-feedback, which adapts the gain of P and D elements depending on the 2-norm of the error $\|\mathbf{e}(t)\|$. The controller's goal is to track a reference function of the outputs and to keep the error within a certain tolerated accuracy λ. This kind of λ-tracking in combination with an adaptive controller is described in [19]:

$$\begin{aligned} &\mathbf{e}(t) := \mathbf{l}(t) - \mathbf{l}_{ref}(t) \\ &\mathbf{u}(t) = k(t)\,\mathbf{e}(t) + k(t)\,\kappa\dot{\mathbf{e}}(t) = k(t) \cdot (\mathbf{e}(t) + \kappa\dot{\mathbf{e}}(t)) \\ &\dot{k}(t) = \begin{cases} \gamma \cdot (\|\mathbf{e}(t)\| - \lambda)^2, & \|\mathbf{e}(t)\| \geq \lambda + 1 \\ \gamma \cdot (\|\mathbf{e}(t)\| - \lambda)^{0.5}, & \lambda + 1 > \|\mathbf{e}(t)\| \geq \lambda \\ 0, & (\|\mathbf{e}(t)\| < \lambda) \\ & \quad \wedge (t - t_E < t_d) \\ -\sigma k(t), & (\|\mathbf{e}(t)\| < \lambda) \\ & \quad \wedge (t - t_E \geq t_d) \end{cases} \\ &k(t_0) = k_0 \end{aligned} \tag{5}$$

with $\gamma > 1$, $\kappa > 0$, $\sigma > 0$, $t_d \geq 0$, $\lambda \geq 0$, $k_0 > 0$, determined in pre-simulations and set in Table 4 in Section 5.

Remark 2.2. *It is obvious that the proposed controller is based on the availability of the error velocity. This is sometimes quite hard to arrange, therefore, see [20, 21] for controllers without derivative measurement of the output.*

Controller (5) works as follows: if the error norm is higher than λ, $k(\cdot)$ increases either quadratic or with a square-root function depending on the amount of exceeding the λ-tube. The variable t_E is the point in time, when the error norm latest entered the λ-tube. If the error norm is smaller than λ and t_E is smaller than the parameter t_d, $k(\cdot)$ is staying constant. If the error norm stays within the λ-tube for longer than t_d, there is an exponential decrease of $k(\cdot)$ with decay factor σ.

3. GENERATION OF GAITS

Firstly, it is demonstrated for a worm-like system of 3 mass points, how the controller works and that suitable gaits are necessary. Suitable means some kind of optimality with respect to resting phases of mass points and speed of the whole system. Therefore, arbitrarily chosen reference distance functions $l_{ref,j}(t)$ and their time derivatives $\dot{l}_{ref,j}(t)$ are defined according to [11]:

$$\begin{aligned} l_{ref,1}(t) &= l_0 + \frac{1}{4} l_0 \sin(\omega t) \\ l_{ref,2}(t) &= l_0 + \frac{1}{4} l_0 \sin\left(\omega t + \frac{\pi}{2}\right) \\ \dot{l}_{ref,1}(t) &= \frac{1}{4} l_0 \omega \cos(\omega t) \\ \dot{l}_{ref,2}(t) &= \frac{1}{4} l_0 \omega \cos\left(\omega t + \frac{\pi}{2}\right) \end{aligned} \tag{6}$$

In Fig. 3a can be seen, how the gain $k(t)$ behaves depending on the error norm $\|\mathbf{e}(t)\|$. Considering the worm

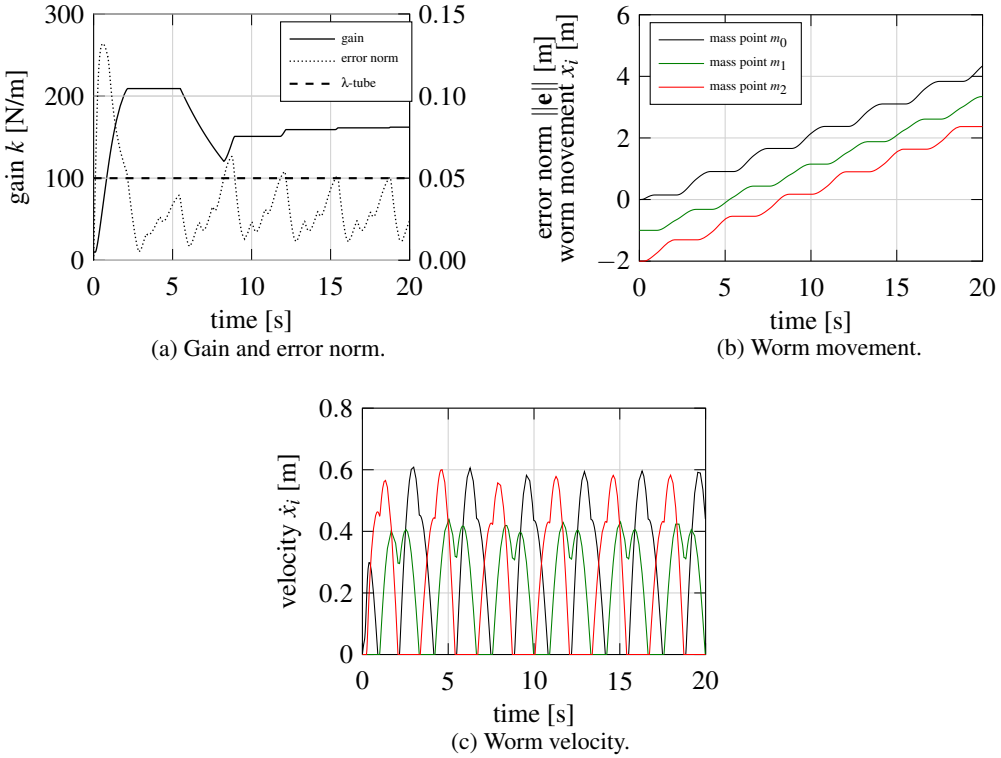

Figure 3: Worm-like locomotion of a system with 3 mass points: arbitrary distance functions (6).

movement $x_i(t)$ in Fig. 3b, the system is able to move forward successfully. However, the velocities of the segments $\dot{x}_i(t)$ are non-uniform, which results in different resting times of the mass points (see Fig. 3c). By using this kind of reference distance functions (6), it is not possible to create a defined gait with a certain sequence of active spikes (i.e., resting mass points), which is important for gait transition. Additionally, the speed of the worm system is rather low due to the arbitrarily chosen gait (keep this in mind for the upcoming simulations, where the speed of the system is increased by using appropriate developed gaits).

Therefore, gaits have to be designed systematically, as described in [22]. For further algorithms relying on binary segment states (contracted, extended), see [13, 23–25].

First of all, gaits differ in the number of active spikes $a \in \{1,\ldots,n\}$. Furthermore, there is a periodic sequence of active spikes $\mathbf{A}(t)$, e.g., for a system with $N = 3$ mass points a possible sequence is $\mathbf{A}(t) = \{1\} \to \{2\} \to \{0\}$. With this knowledge, it can be deduced whether a distance $l_j(t)$ has to be shortened or lengthened at a certain point of time. Following the recommendation from [22], the sequence of active spike should move to left or to the right (only by one segment) like the worm does. A possible sequence is $\mathbf{A}(t) = \{0,1\} \to \{1,2\} \to \{2,3\} \to \{3,0\}$ for a system with $N = 4$ segments, while $\mathbf{A}(t) = \{0,1\} \to \{2,3\} \to \{1,2\} \to \{3,0\}$ is not recommended. Thus, allowed

gaits can be described explicitly by the beginning sequence $\mathbf{A}_0$ of the resting mass points of a time period and the direction *dir* of the wave of active spikes, which can be *"l"* for *left* or *"r"* for *right*.
The reference distance functions are built as described in [22]. The time intervals are defined as:

$$t \in \left[p\frac{T}{N}, (p+1)\frac{T}{N} \right], \quad p \in \mathbf{N}_0.$$

To guarantee a smooth movement of the system, i.e., there are no jerks to the mass points, approximations like $\sin^2(\cdot)$-functions are used to describe the link lengths of the mass points, while $\tau = t - p\frac{T}{N}$:

$$\begin{aligned} \dot{l}_j(\tau) &= \varepsilon l_0 2Nf \sin^2(\pi f N \tau) \\ l_j(\tau) &= l_{0*} + \varepsilon l_0 N f \tau - \frac{1}{2\pi} \varepsilon l_0 \sin(2\pi f N \tau), \end{aligned} \tag{7}$$

- $|\varepsilon| \in (0;1)$ is the relative factor of the maximum distance change,
- f is the frequency of the $\mathbf{A}(t)$-sequence with its periodic time $T = \frac{1}{f}$, chosen in simulation to avoid a rigid-body-movement of the whole worm system,
- $l_0 > 0$ is the initial distance (detensioned spring),
- l_{0*} is the distance at the beginning of the time interval ($\tau = 0$), depending on the previous interval either l_0, $l_0(1+\varepsilon)$ or $l_0(1-\varepsilon)$ [11].

Remark 3.1. *The introduced parameters of the gait generation algorithm are chosen concerning the results in [7] and [22].*

The allowed gaits also differ in their load of the spikes and actuators during operation. Numerical simulations are executed to find the most advantageous (i.e., lowest load of actuators and spikes) gaits for transition. Gaits with equal number of active spikes a (i.e., equally quick) are rated with a weighting function:

$$\begin{aligned} W_{S,g} &:= w_1 {k_{max,S}}^2 + w_2 \sum_{i=0}^{n} {F_{Z,i,max,S}}^2 + w_3 \sum_{j=1}^{n} {u_{j,max,S}}^2 \\ W_{T,g} &:= w_1 {k_{max,T}}^2 + w_2 \sum_{i=0}^{n} {F_{Z,i,max,T}}^2 + w_3 \sum_{j=1}^{n} {u_{j,max,T}}^2 \\ W_{S,g,sc} &:= \frac{W_{S,g}}{W_{S,min}}; \quad W_{T,g,sc} := \frac{W_{T,g}}{W_{T,min}} \\ W_{g,tot} &:= \frac{W_{T,g,sc} + W_{S,g,sc}}{2} + \frac{W_{T,g,sc}}{W_{S,g,sc}} + \frac{W_{S,g,sc}}{W_{T,g,sc}} \end{aligned} \tag{8}$$

Because of transient effects at the beginning of the simulation, this function considers the maximum load of actuators $u_j(\cdot)$ and spikes $F_{Z,i}(\cdot)$, and the maximum gain parameter $k(\cdot)$ for a transient interval $W_{T,g}$ as well as a stationary interval $W_{S,g}$. To have a bigger influence of the load of actuators and spikes, the weighting factors are chosen as:

$$w_1 = 1.0(\mathrm{m/N})^2, \quad w_2 = 4.0\mathrm{N}^{-2}, \quad w_3 = 4.0\mathrm{N}^{-2} \tag{9}$$

Remark 3.2. *These values are individually chosen by the authors and do not underlie a stringent theory, only chosen due to intuition and comprehension of influences on the gait selection: The gain parameter $k(\cdot)$ is an element of the control force $u(t)$, hence, we choose the factor w_3 larger than w_1. Because of the exhaustion of the controllers (actuators) is a pretty unlike effect just like breaking spikes, we choose $w_3 = w_2$. This results in the choice given in the formula above.*
It is obvious, that – at this stage – a more precise investigation of the influence of these weighting factors on the gait selection has to be done, but this was not in the main focus of this work.

Afterwards, the values $W_{S,g}$ and $W_{T,g}$ are scaled to the minimum value $W_{S,min}$ respectively $W_{T,min}$ within the gaits with equal number of active spikes a. Finally, transient and stationary parts are weighted against each other. The minimum value $W_{g,tot}$ within gaits with equal number of active spikes a identifies the most advantageous gait. This leads to the result shown in Table 1-3 for systems with $N = 4, 7, 10$ mass points. These gaits are used for gait transition.

Table 1: Most advantageous gaits for $N = 4$.

a	gait
1	$A_0 = \{1\}, dir = l$
2	$A_0 = \{1,2\}, dir = r$
3	$A_0 = \{3,0,1\}, dir = r$

Table 2: Most advantageous gaits for $N = 7$.

a	gait
1	$A_0 = \{0\}, dir = r$
2	$A_0 = \{0,1\}, dir = r$
3	$A_0 = \{2,3,4\}, dir = r$
4	$A_0 = \{4,5,6,0\}, dir = l$
5	$A_0 = \{3,4,5,6,0\}, dir = l$
6	$A_0 = \{1,2,3,4,5,6\}, dir = l$

Table 3: Most advantageous gaits for $N = 10$.

a	gait
1	$A_0 = \{1\}, dir = r$
2	$A_0 = \{2,3\}, dir = r$
3	$A_0 = \{0,1,2\}, dir = r$
4	$A_0 = \{6,7,8,9\}, dir = l$
5	$A_0 = \{2,3,4,5,6\}, dir = l$
6	$A_0 = \{5,6,7,8,9,0\}, dir = l$
7	$A_0 = \{2,3,4,5,6,7,8\}, dir = l$
8	$A_0 = \{1,2,3,4,5,6,7,8\}, dir = l$
9	$A_0 = \{1,2,3,4,5,6,7,8,9\}, dir = l$

4. GAIT TRANSITION

After determining appropriate gaits via numerical simulations in Section 3, it is now obvious that the locomotion system has to select the most advantageous gait for the actual situation on its own. Thinking of changes of the environment, e.g., change of the slope, malfunction of an actuator or failing of spikes – summarizing an uncertain environment, this gait transition becomes important, because an environmental change results in different loads of (the remaining) actuators and spikes. To react to such circumstances, the system has to change the gait and its frequency autonomously, i.e., on its own. This is addressed to the following investigations.

Remark 4.1. *Analogous example: driving a car – increasing the frequency can be compared to accelerating while gait changing is similar to gear shifting.*

The frequency shall only be changed after concluding a single period, i.e., when a part of the sequence $\mathbf{A}(t)$ is finished. Changing the frequency has a great influence on the loads of actuators and spikes. To adjust the frequency, a P-feedback is used. Additionally, it is possible to weight the load of actuators and spikes against each other using the factors w_{Fz} and w_u:

$$f_1 = \frac{w_{Fz} f_0 \left[1 + k_{p,Fz}(F_{z,soll} - F_{z,ist})\right] + w_u f_0 \left[1 + k_{p,u}(u_{soll} - u_{ist})\right]}{w_{Fz} + w_u} \tag{10}$$

with $k_{p,Fz}$ and $k_{p,u}$ as the gain parameters for spikes and actuators, f_0 as the previous frequency and f_1 as the newly adjusted frequency. The setpoints $F_{z,set}$ and u_{set} are predefined, while the actual values are within a single period:

$$\begin{aligned} F_{z,act} &= \max\{F_{z,0}, F_{z,1}, ..., F_{z,9}\} \\ \bar{u}_j &= \frac{1}{T_e} \int_{t-T_e}^{t} u_j(\tau)\, \mathrm{d}\tau \\ u_{act} &= \max\{\bar{u}_1, \bar{u}_2, ..., \bar{u}_9\} \end{aligned} \tag{11}$$

The value for the frequency has to be limited to f_{max}. Otherwise, there would occur rigid-body-movement, if the frequency exceeded f_{max}, according to [7].

Remark 4.2. *During the period of existence of such rigid-body motion of the whole system, it is uncontrollable in this time-interval.*

This maximum frequency f_{max}, from a kinematical theory according to [7], is given by:

$$f_{max}(a) = \sqrt{\frac{g\sin(\alpha)}{2\pi\varepsilon l_0 N(N-a)}} \tag{12}$$

After finishing a total period T, i.e., when the sequence of active spikes would start again, the system changes the number of active spikes a. The model upshifts (decrease the number of active spikes a), if the maximum frequency f_{max} of a gait is reached. It downshifts (increases the number of active spikes a), if the current reference velocity (13), according to [7], is also reachable with the next slower gait without exceeding the maximum frequency of the slower gait:

$$\bar{v}_{ref}(a,f) = (N-a)\varepsilon l_0 f \tag{13}$$

This downshift frequency f_{min} is:

$$\begin{aligned} & \bar{v}_{min,a} = \bar{v}_{max,a+1} \\ \Leftrightarrow \quad & (N-a)\varepsilon l_0 f_{min} = [N-(a+1)]\varepsilon l_0 f_{max,a+1} \\ \Leftrightarrow \quad & f_{min} = \frac{N-(a+1)}{N-a} f_{max,a+1} \end{aligned} \tag{14}$$

After shifting the gait, the frequency has to be adapted to guarantee the same velocity before and after a gait transition. The analogy to car driving is the adaption of the engine speed while shifting. The frequency after the transition is:

$$\begin{aligned} & \bar{v}_{new} = \bar{v}_{old} \\ \Leftrightarrow \quad & (N-a_{new})\varepsilon l_0 f_{new} = (N-a_{old})\varepsilon l_0 f_{old} \\ \Leftrightarrow \quad & f_{new} = \frac{N-a_{old}}{N-a_{new}} f_{old} \end{aligned} \tag{15}$$

In Fig. 4, the algorithm of frequency control and gait transition is shown, which is executed after the end of the first single period.

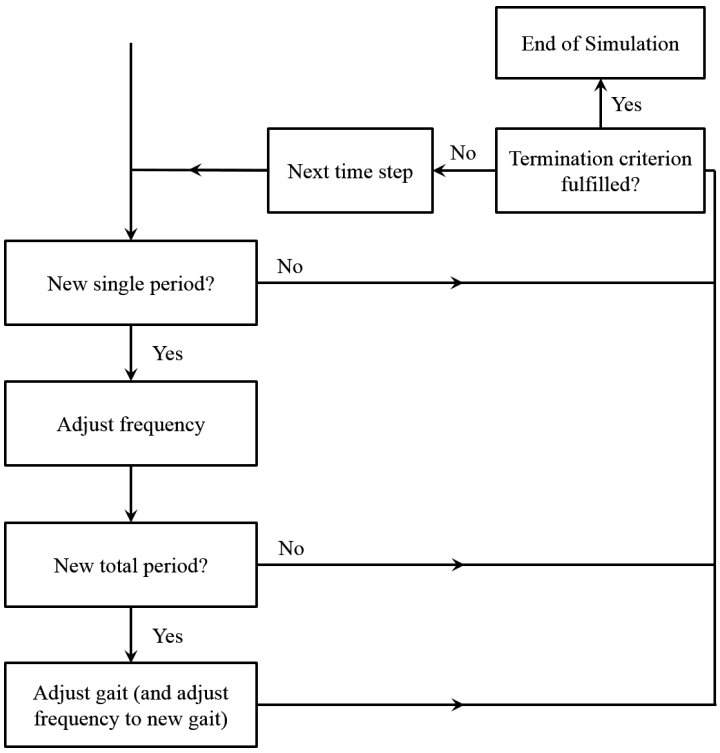

Figure 4: Algorithm of frequency control and gait transition.

5. SIMULATIONS

Example 1: Worm system with constant slope without gait transition: Firstly, a simulation without transition and frequency controlling is shown to get familiar with the basic functionality of the system. The worm crawls up a ramp with a slope of 30° with the maximum frequency $f_{max} = 0.147\text{Hz}$ according to (12) of the fastest gait with $a = 1$. The used parameters for each simulations are shown in Table 4.

Table 4: Parameters for simulations.

$t_{end} = 40\text{s}$	$m_i = 1.0\text{kg}$	$c_j = 10.0\text{N/m}$	$d_j = 5.0\text{kg/s}$
$l_0 = 1.0\text{m}$	$\varepsilon = 0.4$	$\lambda = 0.05\text{m}$	$\kappa = 1\text{s}$
$t_d = 2.0\text{s}$	$\gamma = 500$	$\sigma = 0.2\text{s}^{-1}$	$k_0 = 10\text{N/m}$
$k_{p,Fz} = 0.02\text{N}^{-1}$	$k_{p,u} = 0.02\text{N}^{-1}$	$g = 9.806\text{m/s}^2$	$\alpha = 30°$

Remark 5.1. *As mentioned in Section 2, this set of system's and controller's parameter is arbitrarily chosen. The adaptive nature of the controller is expressed by arbitrary choice of these parameters, because the controller adjusts its behavior to achieve a prescribed control goal of tracking a reference gait. But here, for simulations, it is obvious to choose a set of parameters to present some numerical results.*
The controller data is chosen due to several pre-investigations in [18–20]. The adjustment of some tuning parameters for the controller, like γ, t_d, σ and k_0, was investigated. For example, to large values of t_d makes the controller performance very ponderous. Small values of γ and k_0 decreases the speed of adaptation, meaning the speed of convergence to the finite, necessary gain values for forcing the error into the prescribed λ-tube. Too large values of γ makes the controller behavior very stiff. A large value of σ decreases the level of the gain factor all too fast, which results in a unstable behavior in the λ-tube. Hence, pre-investigations are performed in these references [18–20] and results in the controller parameters in Table 4.

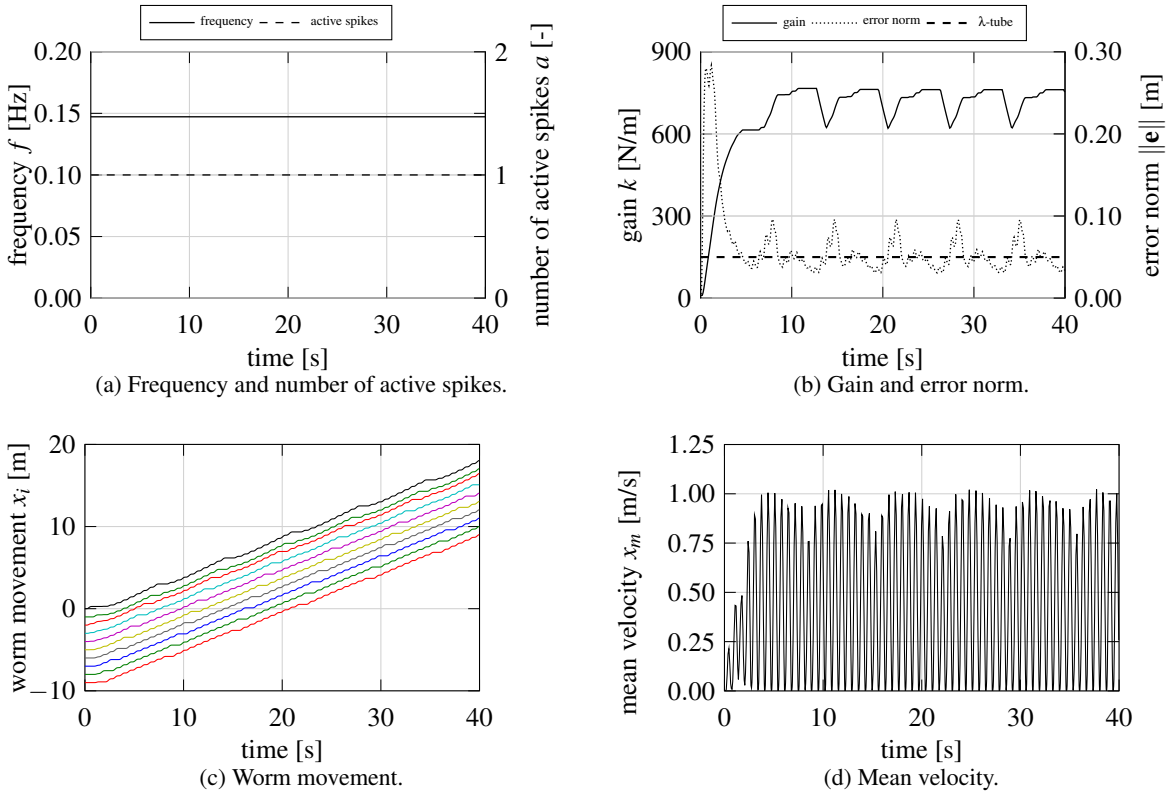

(a) Frequency and number of active spikes.
(b) Gain and error norm.
(c) Worm movement.
(d) Mean velocity.

Figure 5: Worm-like locomotion of a system with 10 mass points: without transition (part 1).

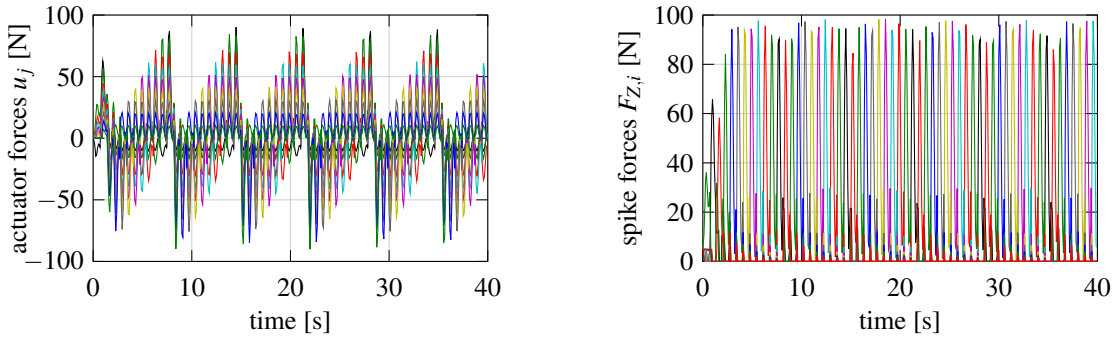

(a) Actuator forces.

(b) Spike forces.

Figure 6: Worm-like locomotion of a system with 10 mass points: without transition (part 2).

One can clearly see in Fig. 5c a typical worm movement with the reference functions according to (7), the first mass point travels 18m in 40s. The adaptive controller works reliably; the gain parameter reaches its stationary state after 7s and oscillates around a value of 700N/m, see Fig. 5b. The maximum spike force is 98.3N, see Fig. 6b, while the maximum actuator force is 90.3N, see Fig. 6a. Thus, the maximum values $F_{Z,max}$ respectively u_{max} are set as 100N for the spike force and 90N for the actuator force for the upcoming simulations *with* gait transitions.

Example 2: Worm system with constant slope and with gait transition: Now, the system will change the gait and the frequency, while the weighing factors in (10) are $w_{Fz} = 1$ and $w_u = 1$. The worm crawls up a ramp with a slope of 30° again.

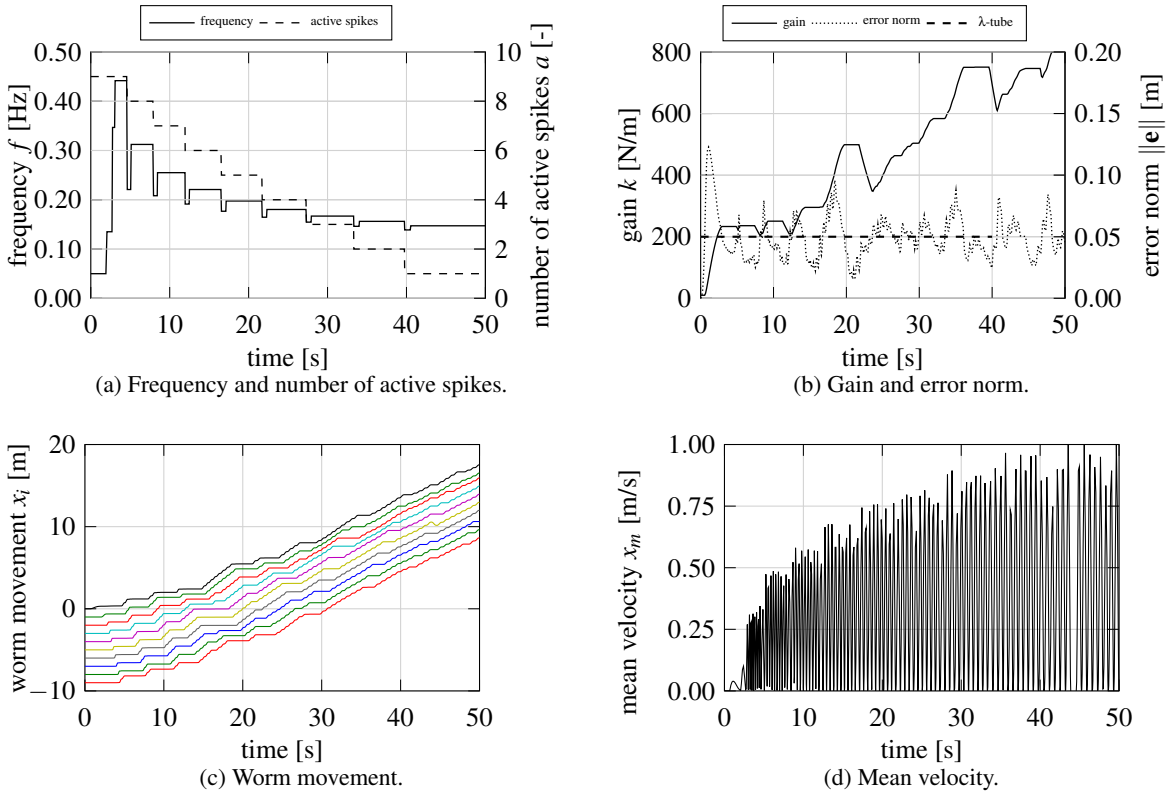

(a) Frequency and number of active spikes.

(b) Gain and error norm.

(c) Worm movement.

(d) Mean velocity.

Figure 7: Worm-like locomotion of a system with 10 mass points: with transition (part 1).

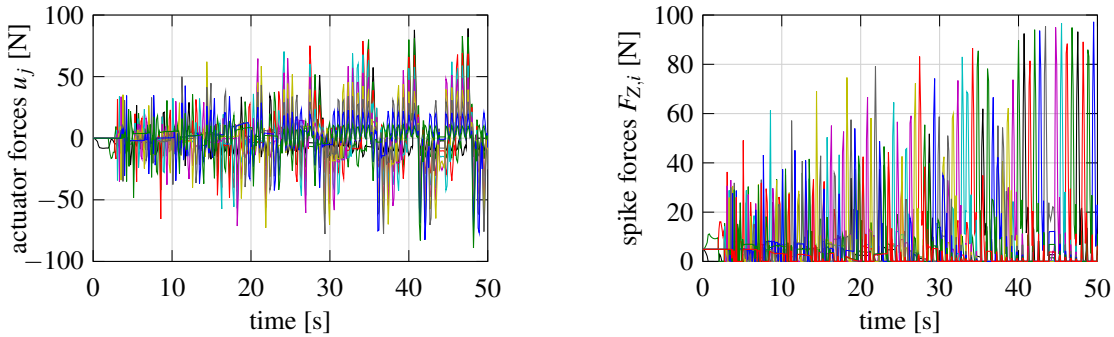

(a) Actuator forces. (b) Spike forces.

Figure 8: Worm-like locomotion of a system with 10 mass points: with transition (part 2).

As expected, the gait is changed depending on the loads, see Fig. 7a. Due to changing only one gait, it takes a long time until the system finds a suitable gait. E.g., the system requires 40s to change from $a = 9$ to $a = 1$. To solve this problem, we restrict the usable number of gaits from 9 to 3 afterwards.

Example 3: Worm system with changing slope and with gait transition: Here, the worm also crawls up a ramp with a slope of 30°, but when the worm covered the mean distance of 25m, there is a change of it to 60° for each segment (in the plots marked with a red vertical line). After a distance of 50m, it is changed to 30° again (also marked with a red vertical line). To get the setpoints $F_{Z,set}$ respectively u_{set} for actuator and spike force, the maximum values $F_{Z,max}$ and u_{max} are multiplied from now on with a safety factor $s = 0.8$. The weighing factors in (10) are $w_{F_Z} = 3$ and $w_u = 1$.
The system adapts the frequency and gait after the change of the slope to reduce/increase the loads of actuators and spikes, see Fig. 9a. Similiar to Example 2, it takes too much time to adjust the gait. E.g., the system requires 53s to change from $a = 3$ to $a = 9$. Furthermore, there occur values above the maximum permissible values $F_{Z,max}$ and u_{max} due to slope of 60°, see Figs. 9b and 9c. This problem is faced below.

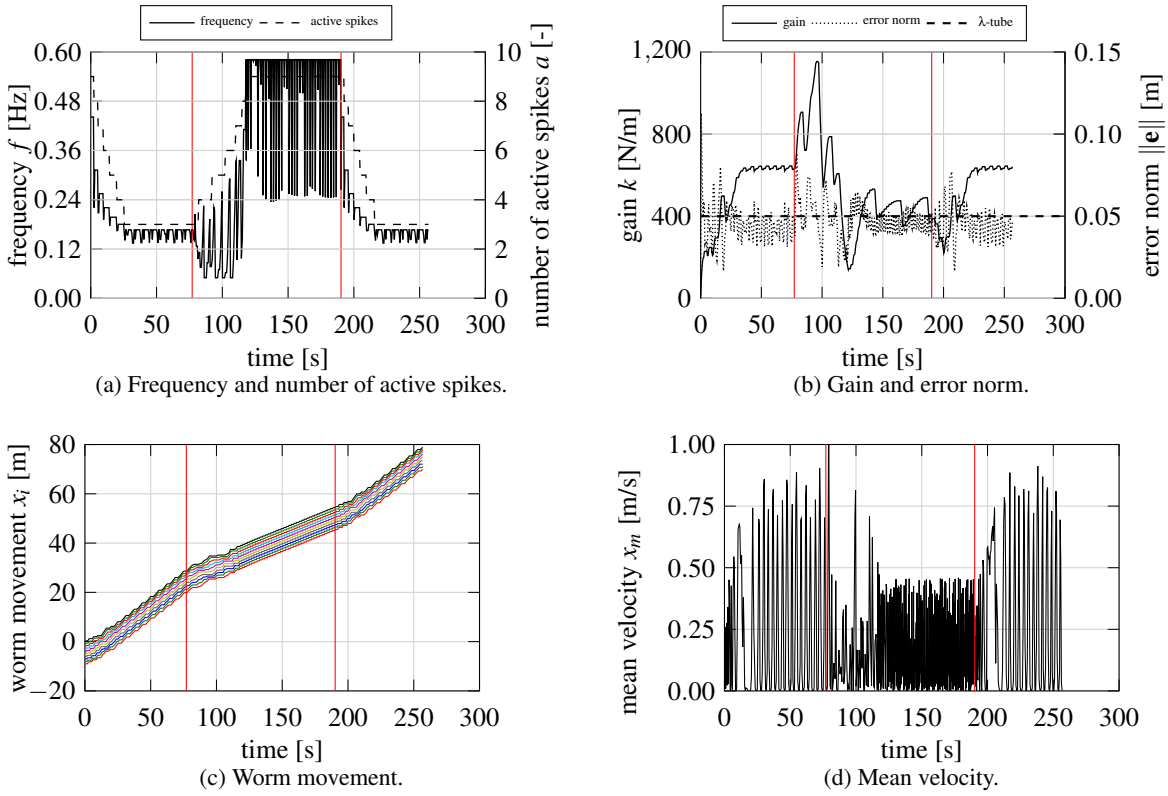

(a) Frequency and number of active spikes. (b) Gain and error norm.

(c) Worm movement. (d) Mean velocity.

Figure 9: Worm-like locomotion of a system with 10 mass points: with transition and changing slope (part 1).

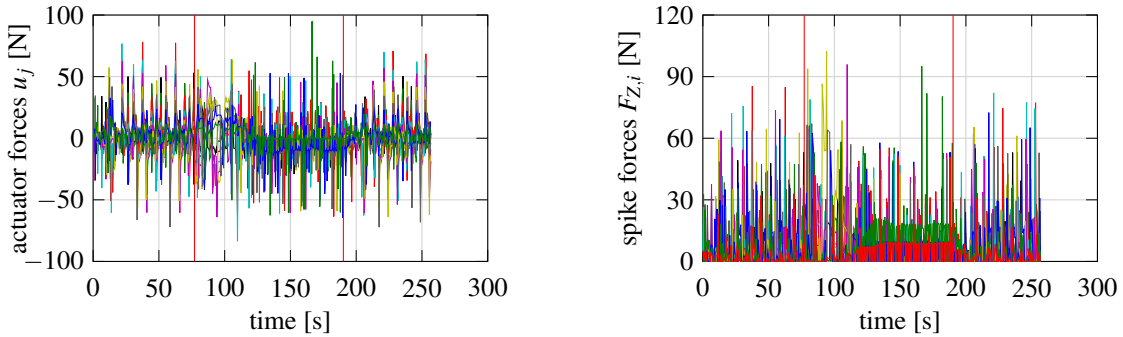

(a) Actuator forces.

(b) Spike forces.

Figure 10: Worm-like locomotion of a system with 10 mass points: with transition and changing slope (part 2).

Example 4: Worm system with changing slope and with gait transition for limitation of actuator forces: To limit the actuator forces, a limitation factor $l = 0.99$ is used, that is multiplied with the maximum actuator force u_{max}. Actuators are now not able to exceed this value. In practice, this could be realized with a current limit function. In contrast, the spike forces cannot be limited by any function and hence, the spike load has to be estimated. The weighing factors in (10) are $w_{Fz} = 1$ and $w_u = 1$.

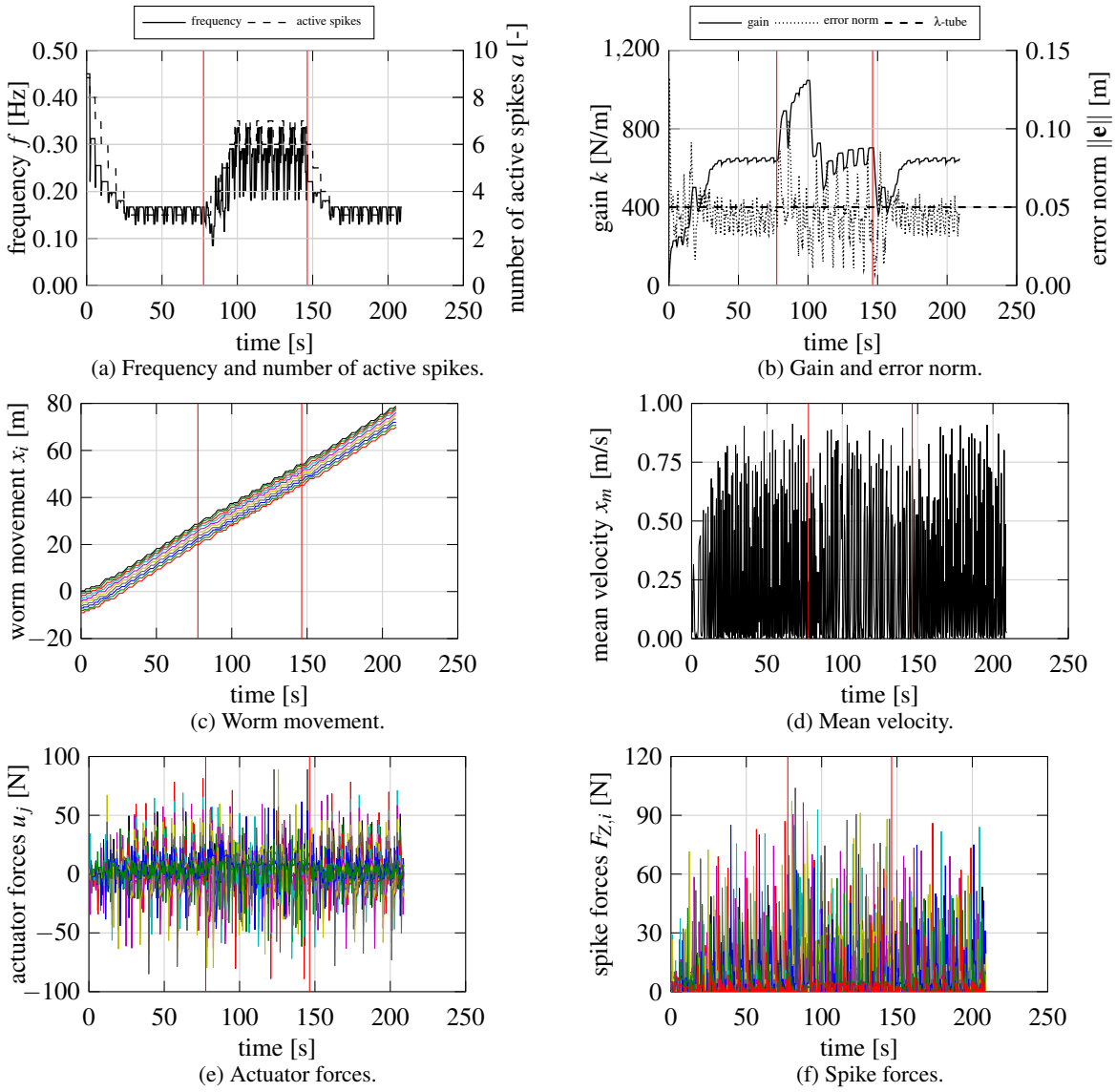

(a) Frequency and number of active spikes.

(b) Gain and error norm.

(c) Worm movement.

(d) Mean velocity.

(e) Actuator forces.

(f) Spike forces.

Figure 11: Worm-like locomotion of a system with 10 mass points: with transition and changing slope.

The actuator forces do not exceed their maximum value, see Fig. 11b. However, the spike forces are still exceeded, see Fig. 11c. Spikes have to be designed adequately solid and should not be overstrained in practice.

Example 5: Worm system with changing slope and with gait transition using only three gaits: As mentioned above, the number of gait transitions has to be reduced. For this purpose, the system can change only three gaits at a time. Possible gaits are now those with $a = 2,5,8$ from Table 4. The weighing factors in (10) are $w_{Fz} = 1$ and $w_u = 3$.

The number of transitions can be reduced significantly with this solution, see Fig. 12a. The system is able to find

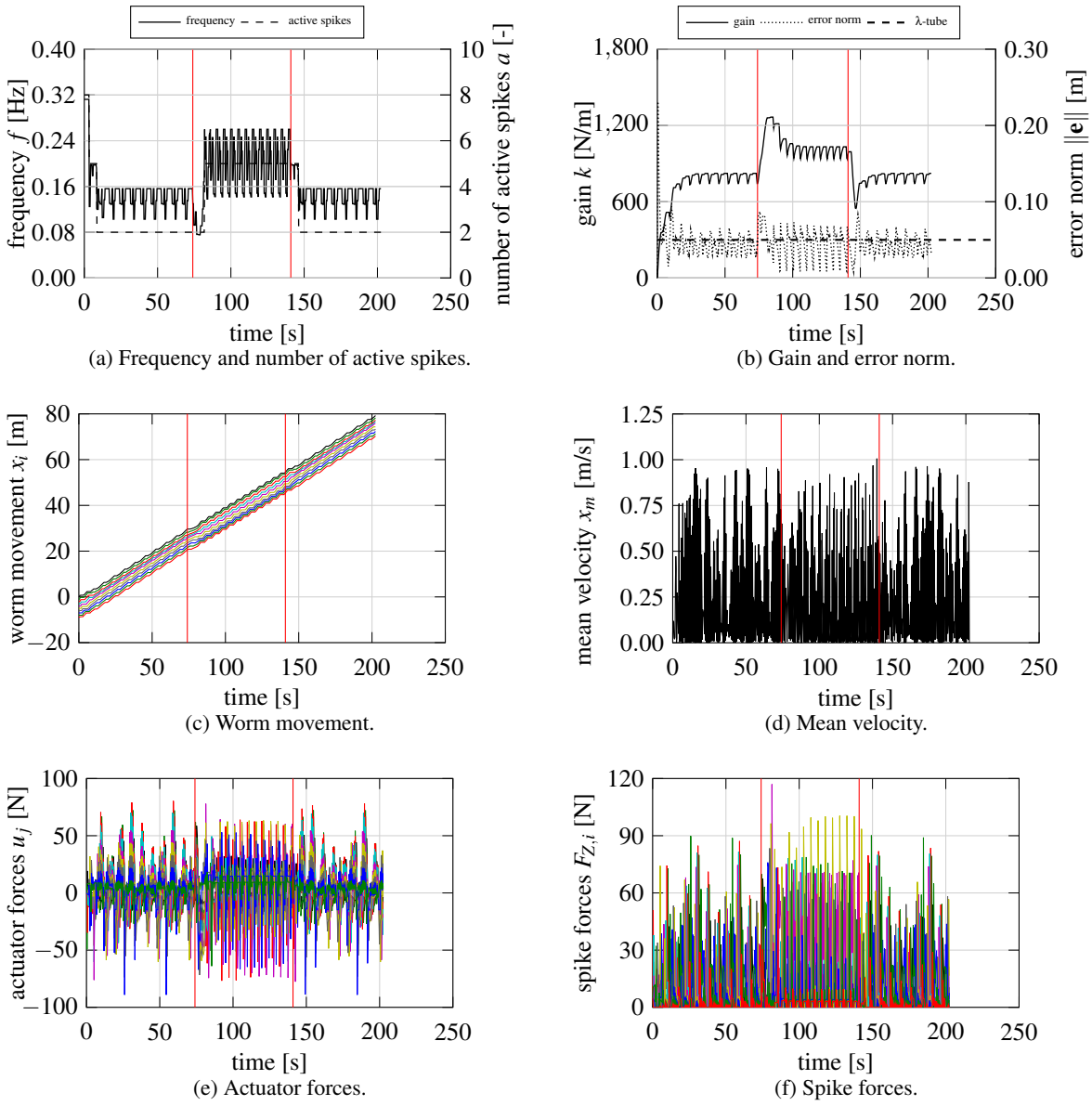

(a) Frequency and number of active spikes.

(b) Gain and error norm.

(c) Worm movement.

(d) Mean velocity.

(e) Actuator forces.

(f) Spike forces.

Figure 12: Worm-like locomotion of a system with 10 mass points: with transition and changing slope.

a suitable gait more quickly. The loads of spikes and actuators are not influenced by this method.

6. CONCLUSION & OUTLOOK

The presented investigations of the dynamical behavior of an artificial locomotion systems focussed on the presentation of a mechanical model for the locomotion system, on the derivation of the model equation describing the dynamic behavior, on the introduction of an adaptive control strategy to control the movement of the system, on the determination and evaluation of most advantageous gaits for a system consiting of 10 mass points, and on a gait transition algorithm adjusting the best gaits to achieve the best possible movement of the system according to

the mean velocity. The gait transition is based on the restriction of the actuator and spike load.
The investigations showed that adaptive control is promising in controlling the neighboring mass point distances to adjust an optimal reference gait to achieve movement of the whole system. The controllers worked successfully and effentively. Moreover, various numerical simulations demonstrated the functionality of the gait transition algorithm in collaboration with a frequency adjusting proportional controller. With respect to the limitation of actuator and spike loads, the system autonomously changed the active gait to fulfill the condition of restriction. This was successfully tested on a system crawling up a ramp with changing slope.
Future work shall be directed to the consideration of sliding friction which has to replace the ideal spiky structure in real experiments; experimental verification of these theoretical investigations; expand the system to a 2D-snake-likemovement based on [26], which deals only with the adaptive movement without gait transition.

7. REFERENCES

[1] G. Miller. The motion dynamics of snakes and worms. *Computer Graphics*, 22:169–173, 1988.

[2] S. Hirose. *Biologically Inspired Robots: Snake-like Locomotors and Manipulators*. Oxford University Press, Oxford, 3rd edition, 1993.

[3] J. Ostrowski and J. Burdick. Gait kinematics for a serpentine robot. *Proc. IEEE Int. Conf. Robotics and Autom.*, 1996.

[4] R. Vaidyanathan, H.J. Chiel, and R.D. Quinn. A hydrostatic robot for marine applications. *Robotics and Autonomous Systems*, 30:103–113, 2000.

[5] W. Liu, A. Menciassi, S. Scapellato, P. Dario, and Y. Chen. A biomimetic sensor for a crawling minirobot. *Robotics and Autonomous Systems*, 54:513–528, 2006.

[6] K. Zimmermann, I. Zeidis, and C. Behn. *Mechanics of Terrestrial Locomotion - With a Focus on Non-pedal Motion Systems*. Springer, Berlin, 2009.

[7] J. Steigenberger and C. Behn. *Worm-like locomotion systems: an intermediate theoretical approach*. Oldenbourg Verlag, 2012.

[8] P. Dario, M.C. Carrozza, B. Allotta, and E. Guglielmelli. Micromechatronics in medicine. *IEEE/ASME Transactions on Mechatronics*, 1:137–148, 1996.

[9] S. Fatikow and U. Rembold. *Microsystem technology and microrobotics.* Springer-Verlag, 1997.

[10] T. Kubota, K. Nagaoka, S. Tanaka, and T. Nakamura. Earth-worm typed drilling robot for subsurface planetary exploration. *IEEE International Conference on Robotics and Biomimetics*, pages 1394–1399, 2007.

[11] S. Schwebke and C. Behn. Worm-like robotic systems: Generation, analysis and shift of gaits using adaptive control. *Artificial Intelligence Research (AIR)*, 2:12–35, 2013.

[12] Rachel Ann Merz and Deirdre Renee Edwards. Jointed setae – their role in locomotion and gait transitions in polychaete worms. *Journal of Experimental Marine Biology and Ecology*, 228:273–290, 1998.

[13] A.B. Slatkin, J. Burdick, and W. Grundfest. The development of a robotic endoscope. *Proc. Int. Conf. Intell. Robots and Systems*, 2, 1995.

[14] P. Meier, J. Dietrich, S. Oberthür, R. Preuß, D. Voges, and K. Zimmermann. Development of a peristaltically actuated device for the minimal invasive surgery with a haptic sensor array. *Micro- and Nanostructures of Biological Systems*, pages 66–89, 2004.

[15] T. Nakamura, T. Kato, T. Iwanaga, and Y. Muranaka. Peristaltic crawling robot based on the locomotion mechanism of earthworms. *Proceedings 4th IFACSympos on Mechatronic Systems*, pages 513–528, 2006.

[16] C. Behn and K. Zimmermann. Straight worms under adaptive control and friction - part 1: Modeling, in iutam symposium on dynamics modeling and interaction control in virtual and real environments. *IUTAM Bookseries*, 30:57–64, 2011.

[17] C. Behn and K. Zimmermann. Straight worms under adaptive control and friction - part 2: Adaptive control, in iutam symposium on dynamics modeling and interaction control in virtual and real environments. *IUTAM Bookseries*, 30:65–72, 2011.

[18] C. Behn. Mathematical modeling and control of biologically inspired uncertain motion systems with adaptive features. Habilitation, Dept. of Mechanical Engineering, TU Ilmenau, Germany, 2013.

[19] C. Behn and P. Loepelmann. Adaptive vs. fuzzy control of uncertain mechanical systems. *International Journal of Applied Mechanics (IJAM)*, 4, 2012.

[20] C. Behn. Adaptive control of straight worms without derivative measurement. *Multibody System Dynamics*, 26(3):213–243, 2011.

[21] X. Ye. Universal λ-tracking for nonlinearly-perturbed systems without restrictions on the relative degree. *Automatica*, 35:109–119, 1999.

[22] J. Steigenberger and C Behn. Gait generation considering dynamics for artificial segmented worms. *Robotics and Autonomous Systems*, 59:555–562, 2011.

[23] I.-M. Chen, S.H. Yeo, and Y. Gao. Gait generation for inchworm-like robot locomotion using finite state model. *Proceedings of the 1999 IEEE International Conference on Robotics & Automation*, 1999.

[24] I.-M. Chen, S.H. Yeo, and Y. Gao. Locomotion gait generation for mutli-segment inchworm. *Proceedings of the 10th World Congress on the Theory of Machines and Mechanisms*, 1999.

[25] I.-M. Chen, S.H. Yeo, and Y. Gao. Locomotive gait generation for inchworm-like robots using finite state approach. *Robotica*, 19:535–542, 2001.

[26] C. Behn, L. Heinz, and M. Krüger. Kinematic and dynamic description of non-standard snake-like locomotion systems. *IFAC Mechatronics*, 2015. doi:10.1016/j.mechatronics.2015.10.010.